

AD_____

Award Number: W81XWH-08-1-0518

TITLE: Molecular MR Imaging of CD44 in Breast Cancer with Hyaluronan-Based Contrast Agents

PRINCIPAL INVESTIGATOR: Dmitri Artemov, Ph.D.

CONTRACTING ORGANIZATION: Johns Hopkins University, Baltimore, MD
21205

REPORT DATE: September 2009

TYPE OF REPORT: Final

PREPARED FOR: U.S. Army Medical Research and Materiel Command
Fort Detrick, Maryland 21702-5012

DISTRIBUTION STATEMENT:

X Approved for public release; distribution unlimited

The views, opinions and/or findings contained in this report are those of the author(s) and should not be construed as an official Department of the Army position, policy or decision unless so designated by other documentation.

REPORT DOCUMENTATION PAGE				Form Approved OMB No. 0704-0188	
<small>Public reporting burden for this collection of information is estimated to average 1 hour per response, including the time for reviewing instructions, searching existing data sources, gathering and maintaining the data needed, and completing and reviewing this collection of information. Send comments regarding this burden estimate or any other aspect of this collection of information, including suggestions for reducing this burden to Department of Defense, Washington Headquarters Services, Directorate for Information Operations and Reports (0704-0188), 1215 Jefferson Davis Highway, Suite 1204, Arlington, VA 22202-4302. Respondents should be aware that notwithstanding any other provision of law, no person shall be subject to any penalty for failing to comply with a collection of information if it does not display a currently valid OMB control number.</small> PLEASE DO NOT RETURN YOUR FORM TO THE ABOVE ADDRESS.					
1. REPORT DATE (DD-MM-YYYY) 01-09-2009		2. REPORT TYPE Final		3. DATES COVERED (From - To) 1 SEP 2008 - 31 AUG 2009	
4. TITLE AND SUBTITLE Molecular MR Imaging of CD44 in Breast Cancer with Hyaluronan-Based Contrast Agents				5a. CONTRACT NUMBER	
				5b. GRANT NUMBER W81XWH-08-1-0518	
				5c. PROGRAM ELEMENT NUMBER	
6. AUTHOR(S) Artemov, Dmitri Zhu, Wenlian				5d. PROJECT NUMBER	
				5e. TASK NUMBER	
				5f. WORK UNIT NUMBER	
7. PERFORMING ORGANIZATION NAME(S) AND ADDRESS(ES) Johns Hopkins University Baltimore, Maryland 21205				8. PERFORMING ORGANIZATION REPORT NUMBER	
9. SPONSORING / MONITORING AGENCY NAME(S) AND ADDRESS(ES) U.S. Army Medical Research Fort Detrick, Maryland				10. SPONSOR/MONITOR'S ACRONYM(S)	
				11. SPONSOR/MONITOR'S REPORT NUMBER(S)	
12. DISTRIBUTION / AVAILABILITY STATEMENT Approved for public release					
13. SUPPLEMENTARY NOTES					
14. ABSTRACT We have synthesized and characterized MR imaging agents using hyaluronic acid (HA) polymer backbones with molecular weights of 16, 31, and 74 kDa. The gadolinium content of HA-(EDA-DTPA-Gd) conjugates varied with preparations and was about ~10% as determined by ICP-MS, which corresponds to ~70% modification ratio of the HA carboxyl groups. T ₁ values of HA-(EDA-DTPA-Gd) prepared from HA of molecular weight 16kD, 31kD, and 74kD and measured at 400MHz were very comparable in the range from 15.3 ms to 19 ms. We also synthesized fluorescent labeled HA probes using the same HA molecules and demonstrated efficient labeling of the polymer using anime-reactive dyes and EDC/EDA linker. Biodistribution of the HA-(EDA-DTPA-Gd) contrast agent in vivo was determined by T1 weighted MRI. Blood half-life time of HA-(EDA-DTPA-Gd) compounds was determined from changes in blood relaxivity as a function of time. Two-compartment pharmacokinetic model provided good fit of experimental data and for 16kDa HA compound the fast and slow phases life times were 12.4 min and 141 min, respectively. Preliminary data suggest an increased uptake of 16 kDa and 31 kDa HA-(EDA-DTPA-Gd) agents in CD44-positive MDA-MB-231 tumor xenografts in comparison to CD44-negative MCF-7 tumors.					
15. SUBJECT TERMS Hyaluronic acid based MR contrast agent. Targeted MRI. CD44 receptors imaging in breast cancer.					
16. SECURITY CLASSIFICATION OF:			17. LIMITATION OF ABSTRACT	18. NUMBER OF PAGES	19a. NAME OF RESPONSIBLE PERSON
a. REPORT	b. ABSTRACT	c. THIS PAGE			USAMRMC
U	U	U	UU	30	19b. TELEPHONE NUMBER (include area code)

Table of Contents

	<u>Page</u>
Introduction.....	4
Body.....	4
Key Research Accomplishments.....	7
Reportable Outcomes.....	7
Conclusion.....	7
References.....	7
Appendices.....	8

Introduction

The major goal of this study is to develop novel single-step CD44 targeting MR imaging probes that can be used to access CD44 status of breast tumors. These probes are based on a natural CD44 ligand, hyaluronic acid (also named hyaluronan, HA), which is a non-sulfated linear glucosaminoglycan composed of 2,000 to 25,000 repeating disaccharide subunits of D-glucuronic acid and N-acetylglucosamine. Functionalized HA decorated with multiple gadolinium groups is used as an efficient targeted MR contrast agent. Experiments have been performed *in vitro* with cultured breast cancer cells and *in vivo* with preclinical mouse models of human breast cancer. This straightforward targeted imaging approach offers advantages over the traditional multiple-step receptor targeting imaging based on monoclonal antibodies or specific peptides.

Body

1. Months 1 – 2.

To synthesize and characterize the hyaluronan (HA)-based contrast agents. Gadolinium contents of the contrast agents will be measured by ICP-MS, and the T1 values will be measured by NMR methods. We will also try to attach a fluorophore tag to the HA backbone for in-vitro cell studies.

During the first year of the project we have synthesized and characterized MR imaging agents using hyaluronic acid (HA) polymer backbones with molecular weights of 16, 31, and 74 kDa. Briefly, HA (200 mg) was dissolved in 2-(N-Morpholino)ethanesulfonic acid buffer (MES 0.1 mol/L, 20 mL, pH 4.75). The carboxyl groups of hyaluronan were activated by the addition of 200mg EDC and 80mg NHS for 30 minutes. 200mg of Ethylenediamine (EDA) was added to this activated hyaluronan solution while pH was maintained at 7.0 with the addition of 1M HCl. The solution was stirred at room temperature for three hours. The product, HA-EDA conjugate, was purified by ultra filtration with an Amicon Centrifugal unit with a 5 or 10kD membrane. Hyaluronan-EDA conjugate was subsequently reacted with 200mg solid DTPA dianhydride in three additions with pH maintained at around 9. This solution was stirred overnight at room temperature. A second batch of 200mg of solid DTPA anhydride was added next day and the reaction proceeded for three more hours. The product, HA-EDA-DTPA conjugate, was purified through ultra filtration with water multiple times. Chelating of gadolinium was performed by the addition of solid GdCl₃. This reaction proceeded overnight at pH=7 in 0.1M citric acid buffer. Final product was purified through ultra filtration with water and lyophilized. The gadolinium content of each HA-(EDA-DTPA-Gd) conjugate varied with preparations. A representative gadolinium content of one of these conjugate was 10% as determined by ICPMS, which corresponds to about 70% of the carboxyl groups of HA being attached to EDADTPA- Gd. T1 values of the HA-(EDA-DTPA-Gd) conjugates were measured at 400 MHz at the concentration of in-vivo injection, which is 40mg/ml in deionized water. T1 values of HA-(EDADTPA- Gd) prepared from HA of molecular weight 16kD, 31kD, and 74kD were very comparable in the range from 15.3 ms to 19 ms.

2. Months 3 - 7.

In-vitro studies will be performed on commercially available human breast cancer cell lines, MDA-MB-231 and Hs578T that expresses CD44. The binding of fluorophore tagged HA to both type of cancer cells will be examined by a fluorescence microscope. Best binding conditions will be investigated. CD44 negative human breast cancer cells MCF-7 and BT-474 will be used as a negative control. HA of different molecular weights will be compared for the binding effectiveness.

Fluorescent labeled HA probes were synthesized using two alternative strategies. Firstly, Alexa-Fluor488 aminoreactive dye (Invitrogen) was used to modify Hyaluronan-EDA conjugates. The reaction was carried out at room temperature and pH=9 using 3X molar excess of the fluorescent probe. Final product was purified by ultrafiltration using 15 kDa cutoff centrifuge filter devices. In a second approach, a fluorescent hyaluronan (MW 31kD) conjugate was synthesized by reacting hyaluronan with carboxylic reactive BODIPY® FL hydrazide (Molecular Probes D2371) in the presence of EDC and sulfur-NHS. Briefly, 40 mg of HA was reacted with 0.5 mg BODIPY® FL for 0.5 hours in 4 ml of 0.1 M 2-(N-Morpholino)ethanesulfonic acid buffer (MES) in the presence of 10 mg of N-(3-dimethylaminopropyl)-N-ethylcarbodiimide hydrochloride (EDC) and 10 mg of N-hydroxysuccinimide (NHS) at pH = 5.4. Final product was purified through ultrafiltration. The

fluorescent yield was significantly higher for the direct conjugation strategy and, therefore, BODIPY fluorescent HA conjugates (HA-BODIPY) were used in cell studies.

FACS experiments were performed with cultured MDA-MB-231 cells (high CD44 expression level) and MCF-7 (low CD44 levels). Scatter plots of the specific fluorescence per cell for MCF-7 and MDA-MB-231 cells labeled with 31 kDa HA-BODIPY are presented in Fig.1. CD44-negative BT-474 cells demonstrated similarly low staining efficiency comparable to MCF-7 cells.

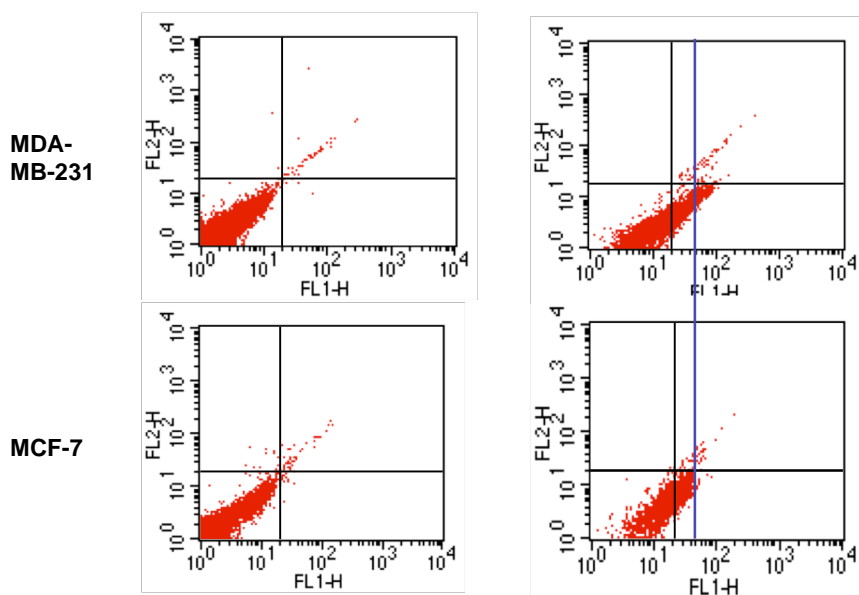


Figure 1. Cells treated with 0.15 mg/ml 31 kDa HA-BODIPY conjugate (right). Left are the untreated control cells.

Top: MDA-MB-231, bottom: MCF-7.

A significant increase in the number of labeled cells was detected for CD44-expressing MDA-MB-231 breast cancer cells. Relative populations of strongly labeled cells calculated as a sum of upper right (UR) and lower right (LR) quadrants were ~37% for MCF-7 and ~47% for MDA-MB-231 cells, respectively (see table below).

File: MCF7HA5.010			File: 231HA5.002		
Acquisition Date: 14-Sep-09			Acquisition Date: 14-Sep-09		
Quad	Events	% Gated	Quad	Events	% Gated
UL	1	0.04	UL	0	0.00
UR	36	1.27	UR	69	1.16
LL	1774	62.46	LL	3144	52.88
LR	1029	36.23	LR	2732	45.95

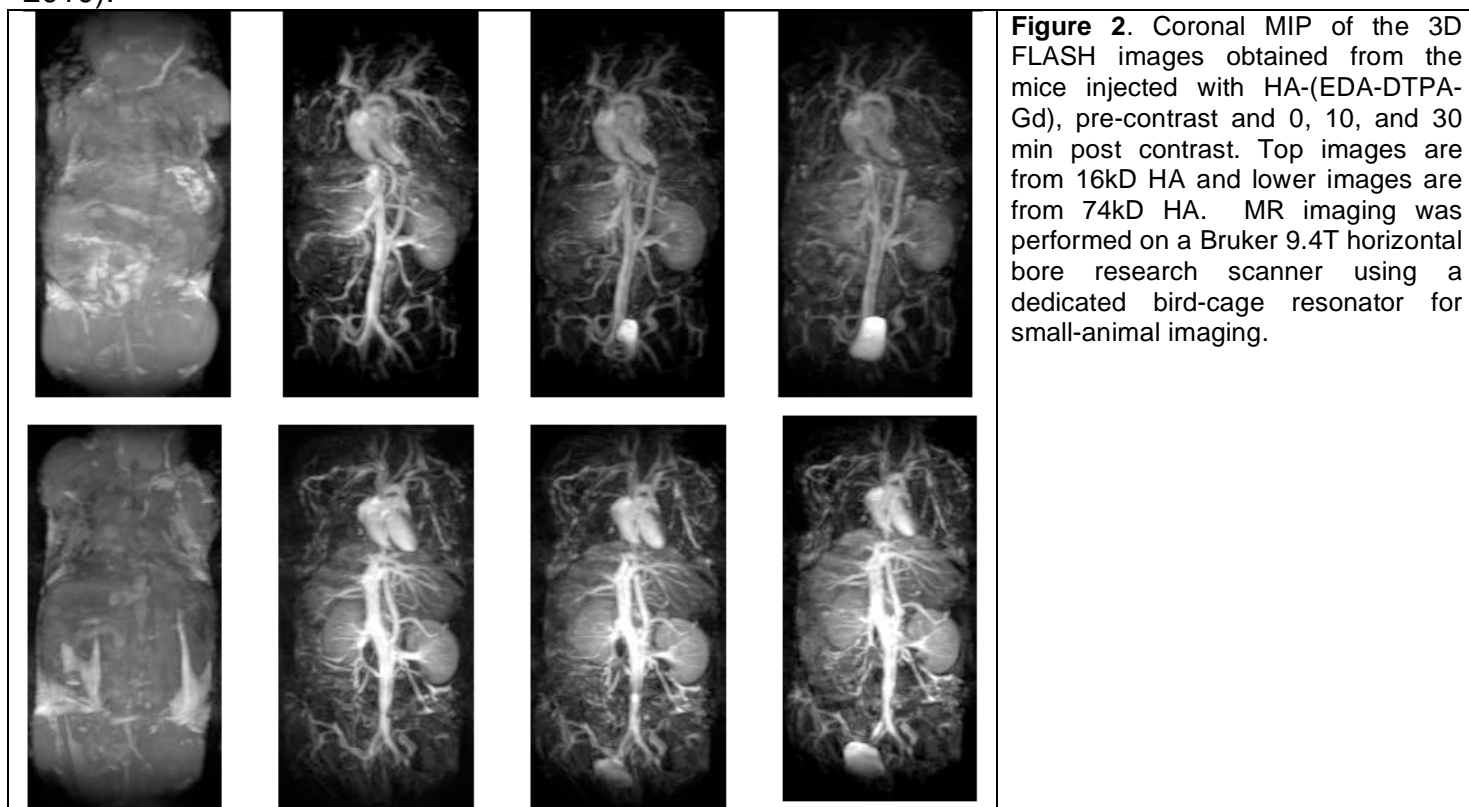
3. Months 8-12.

In vivo biodistribution and plasma pharmacokinetics of HA conjugates will be measured with fluorescent assays of homogenized organs and blood samples respectively. The biodistribution and pharmacokinetics studies will be performed with a total of three mice. Contrast enhanced *In vivo* MRI studies by HA gadolinium-DTPA agents will be performed with a total of 6 SCID mice that inoculated bilaterally with MB-231 and MCF-7 tumor xenografts. HA based gadolinium-DTPA agents will be administered by intravenous injection. T1 enhancement of the MDA-MB-231 of high CD44 expression and MCF-7 of low CD44 expression will be compared.

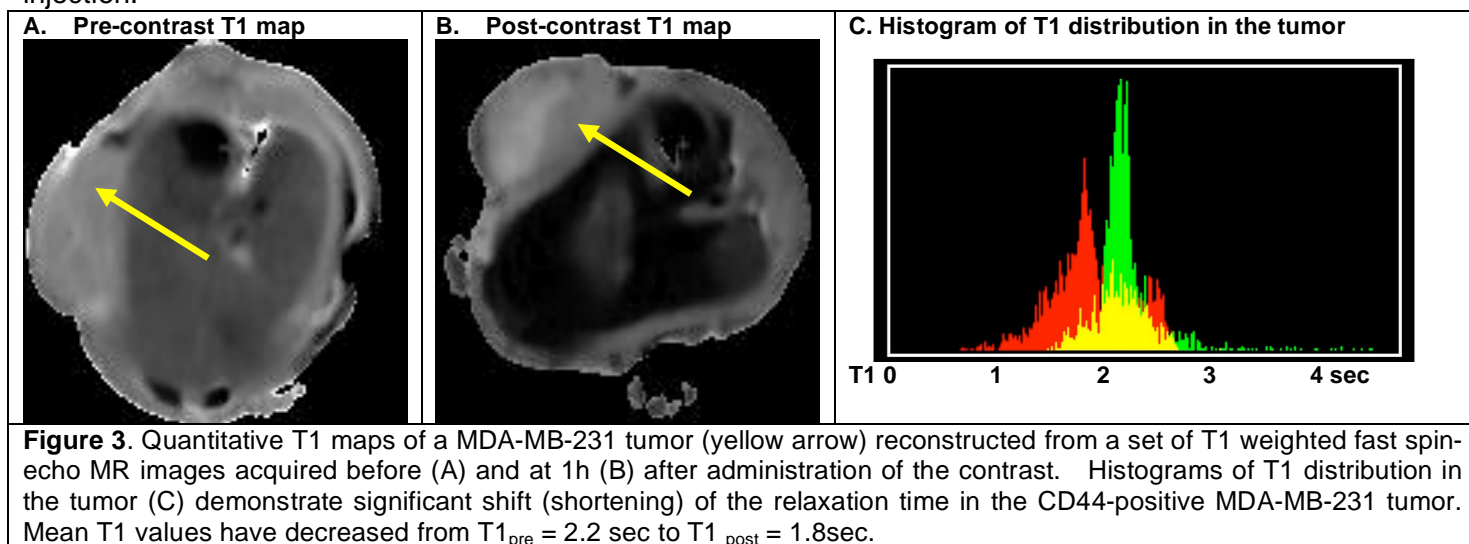
Biodistribution of the HA-(EDA-DTPA-Gd) contrast agent *in vivo* was determined by T1 weighted MRI. Initially, the distribution of the contrast was initially limited to the blood vessels. Eventually, all agents were readily excreted through the kidney to the bladder. 74 kDa HA- (EDA-DTPA-Gd) showed greater detail of the circulatory system, especially in the liver and spleen area. Marked washout was seen for 16 kDa HA-(EDA-DTPA-Gd) after 10 minutes while the washout was barely noticeable for the 74kDa agent, even at 30 minutes. HA-(EDA-DTPA-Gd) of lower molecular weight appeared to be excreted through the kidney faster than its counterpart of higher molecular weight. In addition, HA-(EDA-DTPA-Gd) showed significant uptake by the stomach as early as one hour post injection and 16 kDa HA-(EDA-DTPA-Gd) was absorbed by the stomach faster than 74kDa HA-based compound. At 24h, 16 kDa HA-(EDA-DTPA-Gd) was mostly cleared from the stomach into the lower gastrointestinal tract and feces, while significant uptake at the stomach was observed for 74 kDa HA-(EDA-DTPA-Gd). Overall, no adverse reactions such as weight loss and death were observed in mice received HA-(EDA-DTPA-Gd). Typical MR imaging data are presented in Fig. 2.

Blood half-life time of HA-(EDA-DTPA-Gd) compounds was determined from changes in blood relaxivity as a function of time. Two-compartment pharmacokinetic model provided good fit of experimental data and for 16kDa HA compound the fast and slow phases life times were 12.4 min and 141 min, respectively. Over 64% of the HA-(EDA-DTPA-Gd) based on 16 kDa injected was cleared during the fast phase. Preliminary data suggest an increased uptake of 16 kDa and 31 kDa HA-(EDA-DTPA-Gd) agents in CD44-positive MDA-MB-231 tumor xenografts in comparison to CD44-negative MCF-7 tumors. Please see a detailed description of the

experimental design and results in the attached manuscript (In press, *Contrast Media and Molecular Imaging*, 2010).



T1 weighted MR images and reconstructed pixel by pixel T1 maps of the MDA-MB-231 tumor measured before and at 60 min after administration of HA-(EDA-DTPA-Gd) (MW of 16 kDa, at a dose of 320 mg/kg, i.v.) are shown in Fig. 3. A significant reduction in tumor T1 values was detected in the tumor starting from 30 min post injection.



Key Research Accomplishments

- Paramagnetic HA-based contrast agents were synthesized and characterized
- Fluorescent analogs of HA-conjugates were synthesized and tested in in vitro cultured breast cancer cell systems
- Pharmacokinetics and biodistribution of the HA-(EDA-DTPA-Gd) agents were defined in vivo in

mouse models of human breast cancer.

- In vivo MRI experiments with CD44-positive and CD44-negative breast cancer models were initiated.

Reportable Outcomes

1. Wenlian Zhu, Zaver M. Bhujwalla, and Dmitri Artemov. "Biocompatible Blood Pool MRI Contrast Agents Based on Hyaluronan". Revised version in Contrast Media and Molecular Imaging, 2010.
2. Wenlian Zhu, Dmitri Artemov. "Potential Application of Hyaluronic Acid in MR Imaging". ISMRM 17-th Scientific Meeting, 3139, Honolulu, 18-24 April 2009.

Conclusion

The synthesized targeted MR contrast agents demonstrate very good T1 relaxivity that translates to good signal-to-noise ratio for MR imaging experiments. Preliminary data suggest preferable binding of the constructs to CD44 expressing breast cancer cells that represent aggressive and potentially most lethal subpopulation in breast cancer. Based on our results HA carriers labeled with both Gd groups for MR imaging and cytotoxic moieties can be used as a unique biocompatible platform for theranostic applications in breast cancer.

List of Personnel

PI: Dmitri Artemov, Ph.D.

Fellow: Wenlian Zhu, Ph.D.

References

1. Toole, B. Hyaluronan: from extracellular glue to pericellular cue. Nat Rev Cancer. 2004 Jul;4(7):528-39.
2. Shipitsin M, Campbell LL, Argani P, Weremowicz S, Bloushtain-Qimron N, Yao J, Nikolskaya T, Serebryiskaya T, Beroukhim R, Hu M, Halushka MK, Sukumar S, Parker LM, Anderson KS, Harris LN, Garber JE, Richardson AL, Schnitt SJ, Nikolsky Y, Gelman RS, Polyak K. Molecular definition of breast tumor heterogeneity. Cancer Cell. 2007 Mar;11(3):259-73.
3. Ailles LE, Weissman IL. Cancer stem cells in solid tumors. Curr Opin Biotechnol. 2007 Oct;18(5):460-6.
4. Eliaz RE, Szoka FC Jr. Liposome-encapsulated doxorubicin targeted to CD44: a strategy to kill CD44-overexpressing tumor cells. Cancer Res. 2001 Mar 15;61(6):2592-601.
5. Auzenne E, Ghosh SC, Khodadadian M, Rivera B, Farquhar D, Price RE, Ravoori M, Kundra V, Freedman RS, Klostergaard J. Hyaluronic acid-paclitaxel: antitumor efficacy against CD44(+) human ovarian carcinoma xenografts. Neoplasia. 2007 Jun;9(6):479- 86.
6. Iyer AK, Khaled G, Fang J, Maeda H. Exploiting the enhanced permeability and retention effect for tumor targeting. Drug Discov Today. 2006 Sep;11(17-18):812-8.
7. Banerji S, Wright AJ, Noble M, Mahoney DJ, Campbell ID, Day AJ, Jackson DG. Structures of the Cd44-hyaluronan complex provide insight into a fundamental carbohydrate-protein interaction. Nat Struct Mol Biol. 2007 Mar;14(3):234-9.
8. Popot MA, Bonnaire Y, Guéchet J, Toutain PL. Hyaluronan in horses: physiological production rate, plasma and synovial fluid concentrations in control conditions and following sodium hyaluronate administration. Equine Vet J. 2004 Sep;36(6):482-7.

Appendices

Please see attached manuscript submitted to Contrast Media and Molecular Imaging (revised version)

Biocompatible Blood Pool MRI Contrast Agents Based on Hyaluronan

Wenlian Zhu and Dmitri Artemov

JHU ICMIC Program, The Russell H. Morgan Department of Radiology and Radiological Science, Johns Hopkins University School of Medicine, Baltimore, MD 21205 U.S.A.

Grant Support: National Cancer Institute/NIH P50 CA103175, DOD Breast Cancer Concept Grant, and Maryland Stem Cell Research

Corresponding Author: Dmitri Artemov

Phone: (410) 614-2703

Fax: (410) 614-1948

E-mail: dmitri@mri.jhu.edu

Running head: Hyaluronan based blood pool contrast agents.

Key words: hyaluronan, biocompatible contrast agents, magnetic resonance angiography.

ABSTRACT

Biocompatible gadolinium blood pool contrast agents based on a biopolymer, hyaluronan were investigated for magnetic resonance angiography application. Hyaluronan, a non-sulfated linear glucosaminoglycan composed of 2,000 to 25,000 repeating disaccharide subunits of D-glucuronic acid and N-acetylglucosamine with molecular weight up to 20 mDa, is a major component of the extracellular matrix. Two gadolinium contrast agents based on 16 kDa and 74 kDa hyaluronan were synthesized, both with R1 relaxivity around $5\text{mM}^{-1}\text{s}^{-1}$ per gadolinium at 9.4 Tesla. These two hyaluronan based agents show significant enhancement of the vasculature for an extended period of time. Initial excretion was primarily through the renal system. Later uptake was observed in the stomach and lower gastrointestinal tract. Macromolecular hyaluronan based gadolinium agents have a high clinical translation potential as hyaluronan is already approved by FDA for a variety of medical applications.

INTRODUCTION

Blood pool contrast agents (BPCA) are desirable in applications such as magnetic resonance angiography (MRA) and tumor microvasculature characterization. In comparison to the commonly used extracellular MRI contrast agents such as gadopentetate dimeglumine, BPCAs exhibit lower leakage into the interstitial space, which minimizes non-specific soft tissue enhancement while prolonging the plasma half-life. These characteristics, in combination with higher relaxivity, can provide better contrast for blood vessels as compared to the standard small molecular extracellular contrast agents such as Gd-DTPA. Relative to normal tissues, solid tumors have enhanced permeability and retention of macromolecules (1). Thus, BPCAs based on macromolecules are also well suited to assess tumor angiogenesis due to these tumor specific properties.

One way to attain prolonged blood circulation time is to design BPCAs as either small molecules that bind to serum albumin, or macromolecules. Currently, there is only one blood pool MRI contrast agent, gadofosveset trisodium, that has been approved for clinical MRA application in Europe (2). Gadofosveset trisodium is also approved by the FDA in the United States to evaluate aortoiliac occlusive disease in adults with known or suspected peripheral vascular complication. Gadofosveset trisodium is a small molecule that reversibly binds to blood serum albumin, which has been proven to be beneficial for MRA applications. However, the properties of macromolecular BPCAs make them better suited for studies aimed at quantifying tumor microvasculature as ambiguities related to reversible albumin binding dynamics are avoided (3). Many macromolecular blood pool agents under current development have shortcomings because of a lack of biocompatibility, toxicity, immunogenicity (4,5), and slow excretion, which eventually can result in the accumulation of toxic Gd^{3+} ions (6-8). An ideal macromolecular BPCA needs to be large enough so that it has a prolonged blood circulation time and yet small enough to pass through the kidney for unhindered excretion. It has been reported that the vascular permeability in normal tissues of macromolecules with molecular weight greater than 50 kDa is very limited, while the ultrafiltration threshold of the kidney glomerular membrane is below the size of blood serum albumin, a globular protein of 67 kDa (9). If the molecular size was the only determining factor, it would appear that molecules with molecular weight between 50 and 65 kDa would be most suitable blood pool contrast agent candidates. They would remain in the circulation for an extended period of time, and eventually would be eliminated through the

kidneys. However, other factors, such as charge, shape, and hydrophilic/lipophilic balance also affect the extravasation and excretion rates of macromolecules. Generally, amphipathic organic anions with a relatively high molecular weight are eliminated by the liver via metabolism and/or biliary excretion while small and hydrophilic organic anions are excreted into the urine (10). Relative unhindered clearance through the kidneys may be achieved by using hydrophilic agents with limited protein binding.

Hyaluronan (HA) is a suitable macromolecule platform for developing blood pool contrast agents. HA is a natural linear polysaccharide composed of alternating (β -1,4)-linked d-glucuronic acid and (β -1,3) N-acetyl-d-glucosamine residues with molecular weights as high as 10^7 dalton. HA is widely distributed in the extracellular matrix of connective tissues of animals and plays a role in organ structural stability and tissue organization. It is biocompatible and non-immunogenic. HA is readily available in a wide range of defined molecular weights through microbial fermentation (11,12). Due to its unique viscoelastic rheological properties and safety profile, HA has been utilized in a broad range of medical applications such as ophthalmology, orthopedic surgery and rheumatology, otolaryngology, dermatology and plastic surgery, surgery and wound healing, and pharmacology and drug delivery (13). More significantly, Hyaluronic Acid Chemotransport Technology (HyACT[®]), in which anti-cancer drugs are entrained in an HA matrix, has entered human clinical trials (14). HA is naturally biodegradable since it is digested by a series of enzymatic reactions *in-vivo* that generate polysaccharides of decreasing sizes, which in principle may facilitate the timely excretion of HA based macromolecular contrast agents. In this study, we used HA of molecular weight 16kDa and 74kDa, which contain approximately 40 and 183 repeating disaccharide subunit respectively, as macromolecular backbone carriers for Gd-DTPA groups. We assessed the enhancement pattern of these HA and Gd-DTPA complex as blood pool agents, and compared them to another common preclinical macromolecular blood pool MRI contrast agent, a bovine serum albumin Gd-DTPA complex (15,16).

MATERIALS AND METHODS

Materials

Hyaluronan with molecular weights of 16 and 74 kDa were obtained from Lifecore Biomedical (Chaska, Minnesota). N-(3-dimethylaminopropyl)-N-ethylcarbodiimide hydrochloride (EDC) and N-hydroxysuccinimide (NHS) were from Pierce (Rockford, IL). Other reagents were

obtained from Sigma-Aldrich (St. Louis, MO). All reagents were used without further purification. SCID mice were purchased from NCI with body weight ranged from 21 to 25 gram.

Synthesis of hyaluronan-EDA -diethylenetriaminepentaacetic acid-gadolinium (HA-EDA-DTPA-Gd).

HA-(EDA-Gd-DTPA) was synthesized with a modified method described earlier (17,18). All conjugation reactions were carried out at room temperature. Briefly, 200 mg of HA of different molecular weights (0.5 mmol of disaccharide monomer subunit) was dissolved in 2-(N-Morpholino)ethanesulfonic acid buffer (MES 0.1 mol/L, 20 mL, pH 4.75). The carboxyl groups of hyaluronan were activated by the addition of 200 mg (1.04 mmol) EDC and 80 mg (0.70 mmol) NHS for 30 minutes. 200 mg (3.3 mmol) of Ethylenediamine (EDA) was added to this activated hyaluronan solution while pH was maintained at 7.0 with the addition of 1M HCl. This solution was stirred at room temperature for three hours. The product, HA-EDA conjugate, was purified by ultrafiltration with an Amicon Centrifugal unit with a 5 or 10 kDa membrane.

Hyaluronan-EDA conjugate was subsequently reacted with 200 mg (0.56 mmol) solid DTPA dianhydride in three additions in 40 ml 0.1M HEPES buffer while pH was maintained at around 10 with the addition of 1M NaOH. This solution was stirred overnight at room temperature. A second batch of 200 mg solid DTPA anhydride was added next day and the reaction proceeded for three more hours. The product, HA-(EDA-DTPA) conjugate, was purified through ultrafiltration with water multiple times. Chelating of gadolinium was performed with the addition of 500 mg solid $\text{GdCl}_3 \cdot 6\text{H}_2\text{O}$ (1.3 mmol). This reaction proceeded overnight at pH 7 in 0.1M citric acid buffer. Final product HA-(EDA-DTPA-Gd) was purified through exhaustive ultra filtration with water and lyophilized.

T₁ Measurement of HA-(EDA-DTPA-Gd) Conjugates

T₁ values of the HA-(EDA-DTPA-Gd) conjugates were measured in deionized water at 25°C. All T₁ Measurements were performed on a horizontal 9.4T Bruker Biospec spectrometer using an inversion – recovery (180 – τ – 90 sequence) method with a fixed T_R of 2000 ms and 9 varying delays of 5, 10, 20, 50, 100, 200, 500, 1000, and 2000 ms. T₁ values were calculated by IDL (Interactive Data Language) using mono-exponential fittings with a linear least-square regression of the fid amplitude.

ICP-MS Measurements

Gadolinium content of the HA-(EDA-DTPA-Gd) conjugates was determined by inductively coupled plasma mass spectroscopy (ICP-MS). HA-(EDA-DTPA-Gd) conjugates were dissolved in 2% element analysis grade nitric acid and diluted to the ICP-MS measurement range, from 5 to 40 µg/L. The gadolinium concentration of this diluted solution was calibrated with a series of ICP-MS standard gadolinium solutions.

Stability Measurements

HA-(EDA-DTPA-Gd) conjugates based on 16 kDa HA at the concentration of 4 mg/ml (Gd concentration 1.1 mM) incubated in RPMI medium that contains 10% fetal bovine serum at pH 6.4, 7.4, and 9.0 respectively over 5 days at 37°C, while T1 values of these solutions were measured at 25 °C at various time points.

In-vivo MRA Studies

All animal experiments were performed in accordance with institutional guidelines. *In-vivo* MRA experiments were performed on a horizontal 9.4T Bruker Biospec spectrometer using a circular volume coil. Mice were anesthetized with an intraperitoneal (i.p.) injection of a ketamine/acepromazine mixture (25 and 2.5 mg/kg, respectively, in saline). For magnetic resonance angiography studies, the tail vein of the mice was catheterized with a 25G needle, which was connected to a T-shape connector that was attached to a HA-(EDA-DTPA-Gd) syringe on one side and a saline syringe (plus 10 international unit Heparin) on the other side. Each syringe was fitted with a stopcock outside the magnet via a 50 cm polyethylene (PE60) catheter tube. HA-(EDA-DTPA-Gd) was given at a dose of 0.1 mmolGd/kg. For comparison, BSA-(DTPA-Gd) was also given at a dose of 0.1 mmolGd/kg. After a triplanar orthogonal scout imaging of the whole body, coronal MRA images were acquired with a three-dimensional fast low-angle shot (FLASH) MR sequence (flip angle 45°, echo time/repetition time 1.85 ms/8 ms, FOV 60x26x26 mm, matrix 128x64x64, number of averages 8) before and after the administration of the contrast agent. The entire acquisition was four-and-half minutes. Data analysis was performed using software developed by the IDL program environment. After 3D apodization and Fourier transformation, all final matrices were zero filled to 256x128x128. Data visualization was through ImageJ (NIH) and Amira (Visage Imaging).

Blood Half Life Studies

Mice were anesthetized with an intraperitoneal (i.p.) injection of a ketamine/acepromazine mixture. HA-(EDA-DTPA-Gd) based on 16kDa HA at a dose of 0.05 mmolGd/kg was injected through the mouse tail vein. About 20 μ l of blood was drawn from the tail vein and collected into a dry and heparinized PCR tube at each time point. T_1 of these blood samples were measured by an inversion recovery method at 25°C. Intrinsic blood T_1 was measured prior to the administration of the contrast agent. The blood relaxivity from HA-(EDA-DTPA-Gd) was obtained after the subtraction of the intrinsic blood relaxivity from the total blood relaxivity at each time point. Fast clearance and slow clearance half-life were calculated with a two phase decay model after the intrinsic blood relaxivity was subtracted.

RESULTS

T_1 values

T_1 values and corresponding relaxivity of HA-(EDA-DTPA-Gd) prepared from HA of molecular weight 16 kDa and 74 kDa in deionized water at 25°C are shown in Table 1. Relaxivity of the individual conjugate was calculated based on these T_1 values, HA-(EDA-DTPA-Gd) concentration and gadolinium content.

Gadolinium content of HA-(EDA-DTPA-Gd) Conjugates

The gadolinium content of each HA-(EDA-DTPA-Gd) conjugate varied slightly with preparations as observed by its T_1 values. The gadolinium content of the conjugates based on 16 kDa and 74 kDa HA used in this report was around 5% of the total weight as determined by ICP-MS, shown in Table 1.

Stability

T_1 values of the HA-(EDA-DTPA-Gd) conjugate based on 16kDa HA in RPMI medium with 10% serum were measure within 5 minutes and up to 5 days at pH 6.3, 7.4, and 9.0. About 5% increase in T_1 was observed at 24 hours in all three pH conditions, and up to 14% increase in T_1 was observed in 5 days, Table 2.

In-vivo MRI Studies

Figure 1 shows a time series of maximal intensity projection (MIP) of the coronal 3D FLASH images obtained from the mice injected with HA-(EDA-DTPA-Gd) based on 16 kDa and 74 kDa HA. The time label of each image is listed as that of the beginning of the acquisition after the injection, and pre-contrast images were subtracted from post-contrast images. For comparison,

results from BSA-(DTPA-Gd), a well tested blood pool contrast agent given at the same gadolinium dose, are also shown in Figure 2. Initially, intense and prolonged enhancement was observed in the vasculature for both HA-(EDA-DTPA-Gd) conjugates and BSA-(DTPA-Gd). However, different distribution and excretion pattern emerged over the next thirty minutes. For HA-(EDA-DTPA-Gd), the distribution of the contrast was initially limited to the blood vessels. HA-(EDA-DTPA-Gd) prepared from HA of molecular weight 74 kDa showed greater detail of the circulatory system, especially in the liver and spleen. Marked washout was seen for HA-(EDA-DTPA-Gd) prepared from 16 kDa HA after 10 minutes while the washout was barely noticeable for the 74 kDa agent, even at 30 minutes (Figure 1). These agents were readily excreted through the kidney to the bladder. HA-(EDA-DTPA-Gd) of lower molecular weight appeared to be excreted through the kidney faster than its counter part of higher molecular weight as shown in Figure 3, images taken 150 minutes after the injection: aorta and vena cava were barely visible for the agent based on 16 kDa while they were still enhanced for the 74 kDa agent. In contrast, no excretion to the bladder was observed for BSA-(DTPA-Gd), which leaked to the extravascular space and eventually into the tissues, especially liver and kidney at 30 minutes post injection. However, HA-(EDA-DTPA-Gd) showed significant uptake by the stomach. HA-(EDA-DTPA-Gd) based on 16 kDa HA was absorbed by the stomach faster than that of 74 kDa. Uptake of 16kDa HA-(EDA-DTPA-Gd) by the stomach was observed as early as one hour post injection, and it was seen in feces 7 hours later (Figure 4). At 24 hours the 16 kDa HA-(EDA-DTPA-Gd) had mostly been cleared from the stomach into the lower gastrointestinal tract and feces while significant uptake at the stomach was still observed for the 74 kDa HA-(EDA-DTPA-Gd) conjugate (Figure 5). Overall, no adverse reactions such as weight loss and death were observed in any mice that received HA-(EDA-DTPA-Gd) conjugates in the following months .

Half Life of HA-(EDA-DTPA-Gd) Based on 16kDa

Figure 6 shows the blood relaxivity of a mouse injected with HA-(EDA-DTPA-Gd) based on 16 kDa HA at various time points after the injection. The change in blood relaxivity as a function of time is best fitted with a two-compartment pharmacokinetic model. The fast phase half time is 12.4 minutes and slow phase half time is 141 minutes. Over 64% of the injected 16 kDa HA-(EDA-DTPA-Gd) was cleared during the fast phase.

DISCUSSION

Since native HA does not have any modifiable amine group, conjugation of DTPA to the carboxyl group of HA was preceded by the introduction of an EDA molecule, a homobifunctional crosslinker with two amine groups. However, following the previously published EDC mediated EDA and HA conjugation methods (17,18), we were not able to obtain a final compound with adequate gadolinium attachment for angiography application. To boost the conjugation between the amine groups of EDA and the carboxyl groups of HA, NHS was added to the HA/EDC solution prior to EDA. Additionally, the amount of EDC added was increased to around two molecular equivalent of HA monomer unit. This process was rather efficient under our experimental conditions, as demonstrated by the gadolinium contents and T_1 of the HA-(EDA-DTPA-Gd) solutions. Although EDA possesses two identical amine groups, the remaining free amine group becomes a weaker base upon the formation of an amide bond at the other amine group with a carboxyl group. The resulting different pK_a (6.86 and 9.92 Handbook of Chemistry and Physics) most likely prevented EDA, a homobifunctional crosslinker from inter- or intra-crosslinking two HA carboxyl groups. After one amine group of the EDA molecule is coupled to a carboxyl group of HA molecule, the second EDA amine group with pK_a of 9.92 is much less likely to be reactive towards another HA carboxyl group at our reaction condition, pH 7. The amount of EDC added to activate the HA carboxyl group is crucial for the high conjugation rate of EDA to HA. Insufficient amount of EDC drastically decreased the EDA-HA conjugation efficiency, and excess amount of EDC increased the amount of a stable adduct formed between EDC and HA (19), thus prevented the subsequent conjugation between EDA and HA.

HA-(EDA-DTPA-Gd) prepared from different molecular weights of HA (16 kDa and 74 kDa) showed comparable gadolinium content, T_1 values at the same concentration of 40 mg/ml, and relaxivity (Table 1). At the same concentration of 40 mg/ml, HA-(EDA-DTPA-Gd) prepared from different molecular weights of HA would contain the same number of disaccharide subunits, and thus the same number of gadolinium attached since the gadolinium content is nearly the same. It appeared that the T_1 relaxation rate of the HA-(EDA-DTPA-Gd) conjugates was determined by the amount of gadolinium present, and not by the molecular weight of the HA carriers at 9.4 Tesla. HA is a linear polymer of repeating disaccharide subunits. An HA molecule assumes an expanded stiffened yet flexible random coil structure in physiological solutions (20), and does not conform to a well defined globular tertiary structure (21).

Consequently, molecular weight of HA seemed to have very little effect on the correlation time of the Gd-DTPA groups and the final relaxivity of the whole conjugate in the molecular weight range used, from 16 to 74 kDa.

Nevertheless, the molecular weight of HA does affect the vascular enhancement pattern of HA-(EDA-DTPA-Gd) conjugates. The higher molecular weight agents provided a stronger and more sustained enhancement to the smaller vessels while the lower molecular weight agents exhibited a higher clearance rate through the kidney. BSA-(DTPA-Gd) was not cleared through the kidney since a normal healthy kidney is able to retain all proteins larger than a molecular mass of 60 kDa. Despite a higher molecular weight than BSA, HA-(EDA-DTPA-Gd) prepared from HA of 74 kDa was partially cleared from the kidney most likely due to its linear structure, which results in an elongated random coil tertiary structure compared to globular proteins of similar molecular weight. However, the longer coil that comes with higher molecular weight did result in a slower kidney excretion, compared to the lower molecular weight counterpart as shown in Figure 1 at 30 minutes, and in Figure 3 at 150 minutes after the administration of the contrast agents. It is not clear how hyaluronidase, which degrades hyaluronan into lower molecular weight fragments (22), affects the clearance of HA-(EDA-DTPA-Gd). Degradation of HA by hyaluronidase is a cellular process that depends on HA receptor such as CD44 (23), or LYVE-1(24). Much of this degradation happens in lymph nodes (24) or liver (25) under normal physiological conditions. Hyaluronidase activity may well be limited when HA-(EDA-DTPA-Gd) remains in the blood circulation. Nevertheless, a Hyaluronan-GdDTPA- agarose beads had been constructed to detect the enhanced hyaluronidase activity of cancer cells by MRI, albeit it was injected subcutaneously in the vicinity of ES-2 ovarian carcinoma tumor xenografts (17).

The *in-vivo* blood distribution of HA-(EDA-DTPA-Gd) based on 16kDa HA followed a biphasic pattern, with a fast phase half time of 12.4 minutes and a slow phase half time of 141 minutes. These results were consistent with the MRA studies: a fast wash-out of this contrast from the vasculature in 10 minutes was observed. In comparison, some common extracellular gadolinium agents have a distribution half life of about five minutes and half elimination time of eighty minutes in human (26). Initial fast blood clearance of HA-(EDA-DTPA-Gd) was probably due to the renal excretion. Overtime, HA-(EDA-DTPA-Gd) leaked into the extravascular space such as stomach and the lower gastrointestinal tract. Elimination entered a slow phase as equilibrium was reached between the renal excretion and gastrointestinal uptake.

HA-(EDA-DTPA-Gd) based on 16kDa HA is fairly stable in serum containing RPMI medium in various pH as shown in Table 2. About 5% and 14% increase in the T_1 values were observed at 24 hours and 5 days, which implied that minor amount of gadolinium was lost from the conjugate during these periods. This loss is consistent with the stability commonly observed for the DTPA-Gd macromolecular complex prepared from cyclic DTPA dianhydride (8,27). The stability of gadolinium containing blood pool agents may be improved by the use of backbone-modified DTPA analogs, wherein all 5 carboxyl groups remained free for metal binding after conjugation to the macromolecules or macrocyclic chelators(8).

Stomach and lower gastrointestinal uptake of HA-(EDA-DTPA-Gd) was not expected. In general, liver or spleen were considered the organs that were involved in the HA metabolism (14). Studies of ^3H labeled HA intravenously injected into sheep showed a concentration dependent half life ranged from 5 to 44 minutes (28). It was also reported that the clearance of ^3H labeled HA was retarded by prior injection of excess unlabelled HA, and renal excretion with an upper limit of 25 kDa played a negligible part in clearance, and the liver was the main site of uptake (29). Fluorescence-labeled-hyaluronan with molecular weight of 800 kDa was reported to have a half life of 42 minutes while liver was shown to play a significant role in its elimination (30). After intravenous injection of a bolus dose of ^{14}C -HA in rabbits, it was shown that 98% of the administered dose had disappeared from the systemic circulation within 6 hours after the administration. Within 100 hours, 63% and 20% of the administered dose was excreted and recovered in the respiratory gas (as $^{14}\text{CO}_2$) or in urine (as low molecular weight HA or monosaccharide fragments). The same authors also reported that the total amount of excretion into bile within 24 hours was reported to be very low, 0.7% of the administered dose, and the total amount of excretion HA into feces, within 100 hours of administration, was also very small, about 0.5% of the administered dose (25)(25). Research on the effects of size and dose of fluorescein-labeled HA on its metabolism has shown that 60% of the tail vein injected 90 kDa HA accumulated in the liver, while both the 3 kDa and 10 kDa fluorescein-labeled HA were quickly excreted in urine with no accumulation in any tissues (31). As such, neither HA nor any other gadolinium based MRI agents administered intravenously are known to have any significant gastrointestinal uptake. The gastrointestinal uptake we observed must be due to the unique structure of our HA-(EDA-DTPA-Gd) conjugates. Additionally, we recognize the fact

that as a bifunctional chelate, DTPA dianhydride has been known crosslinking amines to form higher molecular weight polymeric aggregates(16). In the particular case of HA-EDA, DTPA dianhydride can produce both intramolecular and intermolecular crosslinking that results in a polydispersed HA-EDA-DTPA conjugates. Both types of crosslinking changed the linear structure of HA while intermolecular crosslinking also increased the molecular weight of the final conjugates. Both type of crosslinking may have profound influence on the HA-(EDA-DTPA-Gd) distribution and elimination. We plan to use a bifunctional chelate with only one reactive functional group towards amines such as MX-DTPA (8) in the future to avoid any complication due to the crosslinking.

CONCLUSION

HA-(EDA-DTPA-Gd) has been investigated as blood pool MR contrast agents. Agents based on HA of 16kD and 74kD both show significant enhancement of the vasculature for an extended period of time. Clearance of the HA-(EDA-DTPA-Gd) conjugates based on 16kD HA followed a two phase decay pattern, with a fast phase half life at 12.4 minutes and a slow phase half life at 141.2 minutes, which make them potentially applicable to a range of MR studies including MRA and characterization of the tumor vasculature. Excretion rate of the HA-(EDA-DTPA-Gd) conjugates decreased as the HA molecular weight increased. Uptake in the stomach and lower gastrointestinal tract was observed for the HA-(EDA-DTPA-Gd) conjugates.

Acknowledgement.

We would like to thank Dr. Yoshinori Kato for experimental support, and Dr. Zaver Bhujwala, Dr. Jiangyang Zhang, Dr. Paul Winnard, and Dr. Cong Li for their insightful scientific discussion. Andrew Graham performed the ICP-MS analysis. This work was supported by NIH P50 CA103175, Maryland Stem Cell research, and a DOD Breast Cancer Concept grant W81XWH-08-1-0518.

Table 1 T_1 values (at 40 mg/ml) and relaxivity of HA-(EDA-DTPA-Gd) of different molecular weight at 40 mg/ml at 25°C

MW of HA (kD)	16	74
T_1 values (ms)	16.4	15.3
Gd content (% weight)	4.5	5.2
Relaxivity ($\text{mM}(\text{Gd})^{-1}\text{s}^{-1}$)	5.35	4.96

Table 2 T_1 (ms) of HA-(EDA-DTPA-Gd) conjugate in RPMI medium with 10% FBS at various pH

Time (hour)	pH = 6.3	pH = 7.4	pH = 9.0
0.05	176	194	190
1	178	197	191
2	183	196	194
24	186	208	202
50	190	212	206
123	201	221	220

FIGURE CATION

Figure 1. Coronal maximum intensity projection (MIP) of the 3D FLASH images obtained from the mice injected with HA-(EDA-DTPA-Gd) at 0.1 mmol Gd/kg. Pre-contrast and 0, 10, and 30 minutes post contrast images are shown from left to right. Post-contrast images are shown here after the subtraction of the corresponding pre-contrast images. Top images are from 16kDa HA and lower images are from 74kDa HA.

Figure 2. Coronal MIP of the 3D FLASH images obtained from a mouse injected with BSA-(DTPA-Gd) at 0.1mmol Gd/kg. Pre-contrast and 0, 10, and 30 minutes post contrast images are shown from left to right. Post-contrast images are shown here after the subtraction of the corresponding pre-contrast images.

Figure 3. Coronal MIP of the 3D FLASH images obtained from the mice injected with HA-(EDA-DTPA-Gd) at 150 minutes post injection. Left image is from 16 kDa HA and right image is from 74 kDa HA.

Figure 4. 3D FLASH images obtained from a mouse injected with 16 kDa HA-(EDA-DTPA-Gd), areas with gadolinium uptakes are highlighted. a. and b. axial and coronal images showing the stomach and lower gastrointestinal uptake at 1 hour post injection. c. and d. coronal images showing the lower gastrointestinal and feces uptake at 7 hours post injection. e. a coronal image showing the presence of gadolinium enhancement in the feces at 24 hours.

Figure 5. Coronal MIP of the 3D FLASH images obtained from the mice injected with HA-(EDA-DTPA-Gd) at 24 hour post injection. Left image is from 16 kDa HA and right image is from 74 kDa HA. Highlighted area showed the stomach uptake of 74 kDa HA-(EDA-DTPA-Gd).

Figure 6. Blood relaxivity as a function of time of a mouse injected with 16 kDa HA-(EDA-DTPA-Gd).

REFERENCES

1. Maeda H, Fang J, Inutsuka T, Kitamoto Y. Vascular permeability enhancement in solid tumor: various factors, mechanisms involved and its implications. *Int Immunopharmacol* 2003;3(3):319-328.
2. Goyen M. Gadofosveset-enhanced magnetic resonance angiography. *Vasc Health Risk Manag* 2008;4(1):1-9.
3. Turetschek K, Floyd E, Helbich T, Roberts TP, Shames DM, Wendland MF, Carter WO, Brasch RC. MRI assessment of microvascular characteristics in experimental breast tumors using a new blood pool contrast agent (MS-325) with correlations to histopathology. *J Magn Reson Imaging* 2001;14(3):237-242.
4. Baxter AB, Melnikoff S, Stites DP, Brasch RC. AUR Memorial Award 1991. Immunogenicity of gadolinium-based contrast agents for magnetic resonance imaging. Induction and characterization of antibodies in animals. *Investigative radiology* 1991;26(12):1035-1040.
5. Bogdanov AA, Jr., Weissleder R, Frank HW, Bogdanova AV, Nossif N, Schaffer BK, Tsai E, Papisov MI, Brady TJ. A new macromolecule as a contrast agent for MR angiography: preparation, properties, and animal studies. *Radiology* 1993;187(3):701-706.
6. Frenzel T, Lengsfeld P, Schirmer H, Hutter J, Weinmann HJ. Stability of gadolinium-based magnetic resonance imaging contrast agents in human serum at 37 degrees C. *Investigative radiology* 2008;43(12):817-828.
7. Sieber MA, Lengsfeld P, Frenzel T, Golfier S, Schmitt-Willich H, Siegmund F, Walter J, Weinmann HJ, Pietsch H. Preclinical investigation to compare different gadolinium-based contrast agents regarding their propensity to release gadolinium in vivo and to trigger nephrogenic systemic fibrosis-like lesions. *Eur Radiol* 2008;18(10):2164-2173.
8. Franano FN, Edwards WB, Welch MJ, Brechbiel MW, Gansow OA, Duncan JR. Biodistribution and metabolism of targeted and nontargeted protein-chelate-gadolinium complexes: evidence for gadolinium dissociation in vitro and in vivo. *Magnetic resonance imaging* 1995;13(2):201-214.
9. Takakura Y, Mahato RI, Hashida M. Extravasation of macromolecules. *Adv Drug Deliv Rev* 1998;34(1):93-108.
10. Mizuno N, Niwa T, Yotsumoto Y, Sugiyama Y. Impact of drug transporter studies on drug discovery and development. *Pharmacol Rev* 2003;55(3):425-461.
11. Chong BF, Blank LM, McLaughlin R, Nielsen LK. Microbial hyaluronic acid production. *Appl Microbiol Biotechnol* 2005;66(4):341-351.
12. Guillaumie F, Furrer P, Felt-Baeyens O, Fuhlendorff BL, Nymand S, Westh P, Gurny R, Schwach-Abdellaoui K. Comparative studies of various hyaluronic acids produced by microbial fermentation for potential topical ophthalmic applications. *J Biomed Mater Res A* 2009.
13. Kogan G, Soltes L, Stern R, Gemeiner P. Hyaluronic acid: a natural biopolymer with a broad range of biomedical and industrial applications. *Biotechnol Lett* 2007;29(1):17-25.
14. Brown TJ. The development of hyaluronan as a drug transporter and excipient for chemotherapeutic drugs. *Curr Pharm Biotechnol* 2008;9(4):253-260.
15. Schmiedl U, Ogan M, Paajanen H, Marotti M, Crooks LE, Brito AC, Brasch RC. Albumin labeled with Gd-DTPA as an intravascular, blood pool-enhancing agent for MR imaging: biodistribution and imaging studies. *Radiology* 1987;162(1 Pt 1):205-210.

16. Ogan MD, Schmiedl U, Moseley ME, Grodd W, Paaanen H, Brasch RC. Albumin labeled with Gd-DTPA. An intravascular contrast-enhancing agent for magnetic resonance blood pool imaging: preparation and characterization. *Investigative radiology* 1987;22(8):665-671.
17. Shiftan L, Israely T, Cohen M, Frydman V, Dafni H, Stern R, Neeman M. Magnetic resonance imaging visualization of hyaluronidase in ovarian carcinoma. *Cancer Res* 2005;65(22):10316-10323.
18. Gouin S, Winnik FM. Quantitative assays of the amount of diethylenetriaminepentaacetic acid conjugated to water-soluble polymers using isothermal titration calorimetry and colorimetry. *Bioconjugate chemistry* 2001;12(3):372-377.
19. Kuo JW, Swann DA, Prestwich GD. Chemical modification of hyaluronic acid by carbodiimides. *Bioconjugate chemistry* 1991;2(4):232-241.
20. Cowman MK, Matsuoka S. Experimental approaches to hyaluronan structure. *Carbohydr Res* 2005;340(5):791-809.
21. Blundell CD, Deangelis PL, Almond A. Hyaluronan: the absence of amide-carboxylate hydrogen bonds and the chain conformation in aqueous solution are incompatible with stable secondary and tertiary structure models. *Biochem J* 2006;396(3):487-498.
22. Stern R, Jedrzejewski MJ. Hyaluronidases: their genomics, structures, and mechanisms of action. *Chem Rev* 2006;106(3):818-839.
23. Harada H, Takahashi M. CD44-dependent intracellular and extracellular catabolism of hyaluronic acid by hyaluronidase-1 and -2. *J Biol Chem* 2007;282(8):5597-5607.
24. Jackson DG. Immunological functions of hyaluronan and its receptors in the lymphatics. *Immunol Rev* 2009;230(1):216-231.
25. Lebel L. Clearance of hyaluronan from the circulation. *Advanced Drug Delivery Reviews* 1991;7(2):221-235.
26. Geraldes CF, Laurent S. Classification and basic properties of contrast agents for magnetic resonance imaging. *Contrast Media Mol Imaging* 2009;4(1):1-23.
27. Sherry AD, Cacheris WP, Kuan KT. Stability constants for Gd³⁺ binding to model DTPA-conjugates and DTPA-proteins: implications for their use as magnetic resonance contrast agents. *Magn Reson Med* 1988;8(2):180-190.
28. Lebel L, Fraser JR, Kimpton WS, Gabrielsson J, Gerdin B, Laurent TC. A pharmacokinetic model of intravenously administered hyaluronan in sheep. *Pharm Res* 1989;6(8):677-682.
29. Fraser JR, Laurent TC, Pertoft H, Baxter E. Plasma clearance, tissue distribution and metabolism of hyaluronic acid injected intravenously in the rabbit. *Biochem J* 1981;200(2):415-424.
30. Nakabayashi H, Tsujii H, Okamoto Y, Nakano H. Fluorescence-labeled-hyaluronan loading test as an index of hepatic sinusoidal endothelial cell function in the rat. *International Hepatology Communications* 1996;5(6):345-353.
31. Mochizuki S, Kano A, Shimada N, Maruyama A. Uptake of enzymatically-digested hyaluronan by liver endothelial cells in vivo and in vitro. *J Biomater Sci Polym Ed* 2009;20(1):83-97.

